nature cell biology

p53 induces differentiation of mouse embryonic stem cells by suppressing *Nanog* expression

Tongxiang Lin[1], Connie Chao[1], Shin'ichi Saito[2], Sharlyn J.Mazur[2], Maureen E. Murphy[3], Ettore Appella[2] and Yang Xu[1,4]

The tumour suppressor p53 becomes activated in response to upstream stress signals, such as DNA damage, and causes cell-cycle arrest or apoptosis[1]. Here we report a novel role for p53 in the differentiation of mouse embryonic stem cells (ESCs). p53 binds to the promoter of *Nanog*, a gene required for ESC self-renewal[2,3], and suppresses *Nanog* expression after DNA damage. The rapid down-regulation of *Nanog* mRNA during ESC differentiation correlates with the induction of p53 transcriptional activity and Ser 315 phosphorylation. The importance of Ser 315 phosphorylation was revealed by the finding that induction of p53 activity is impaired in p53^{S315A} knock-in ESCs during differentiation, leading to inefficient suppression of *Nanog* expression. The decreased inhibition of *Nanog* expression in p53^{S315A} ESCs during differentiation is due to an impaired recruitment of the co-repressor mSin3a to the *Nanog* promoter. These findings indicate an alternative mechanism for p53 to maintain genetic stability in ESCs, by inducing the differentiation of ESCs into other cell types that undergo efficient p53-dependent cell-cycle arrest and apoptosis.

Nanog, a homeodomain protein exclusively expressed in ESCs, is required to maintain self-renewal and the undifferentiated state of ESCs[2,3]. *Nanog* expression is rapidly down-regulated during ESC differentiation and the constitutive expression of *Nanog* inhibits ESC differentiation[2,3]. We found that agents that induce DNA damage also down-regulated *Nanog*; to test whether the p53 tumour suppressor might be involved in this process, p53 was activated in ESCs by DNA damage induced by either ultraviolet light (UV) or doxorubicin treatment. These types of DNA damage markedly increased p53 protein levels 4 h after treatment (Fig. 1a, b). At this time point, ESCs did not undergo apoptosis (data not shown). p53-dependent expression of *Mdm2* and *Noxa* was notably increased after DNA damage, indicating that p53 transcriptional activities are activated as early as 4 h after treatment (Fig. 1c, d). Notably, *Nanog* expression was markedly reduced in wild-type ESCs but not in p53$^{-/-}$ ESCs 4 h after DNA damage, indicating that activation of p53 by DNA damage suppresses *Nanog* expression. The reduction in *Nanog* expression after DNA damage was not due to ESC differentiation, because the expression of *Oct3/4* — also exclusively expressed in ESCs and a marker for undifferentiated ESCs[4,5] — remained constant in wild-type ESCs 4 h after treatment (Fig. 1c, d). *Nanog* is also highly expressed in blastocysts, from which ESCs are derived[2,3]. Consistent with the notion that the activation of p53 by DNA damage suppresses *Nanog* expression, the mRNA levels of *Nanog* were also reduced in a p53-dependent manner in mouse blastocysts after treatment with Doxorubicin (Fig. 1e).

We identified two putative p53-binding sites within the *Nanog* promoter region (see Supplementary Information, Fig. S1). One identified p53-binding site, denoted RE1, is located at –871 to –849 relative to the putative translational initiation ATG, and the second site, denoted RE2, is located at –611 to –585. These putative p53 response elements contain a two- and six-nucleotide spacer, respectively, between the two 'half' sites of the p53-binding sites; this feature is consistent with the p53-binding sites involved in p53-dependent transcriptional repression[6]. To confirm that p53 binds to the *Nanog* promoter *in vivo*, chromatin immunoprecipitation (ChIP) was performed to compare the binding affinity of p53 to the *Nanog* promoter with that of the promoters of two well-known p53 target genes, *p21* and *Mdm2*, in ESCs. This analysis showed that a higher percentage of the *Nanog* promoter was bound by p53 than that of the *p21* and *Mdm2* promoters in ESCs (Fig. 2a). To test whether p53 binds specifically to the putative p53-binding sites within the *Nanog* promoter, we cloned the 0.7-kilobase (kb) *Hin*dIII fragment containing the two putative p53-binding sites and mutated the critical cytosine and guanine residues within each p53-binding site to adenine or thymine (see Supplementary Information, Fig. S1). The binding of p53 to the radiolabelled wild-type and mutated (Δp53) *Hin*dIII fragment was determined by McKay assay as described[6]. The results indicate that p53 was bound only to the wild-type *Hin*dIII fragment of the *Nanog* promoter (Fig. 2b). We also performed an electrophoretic mobility shift assay (EMSA) to show that purified p53 bound to oligonucleotides corresponding to the individual wild-type but not mutant RE1 or RE2 sites (Fig. 2c). Together, these findings show that p53 binds specifically to the wild-type RE1 and RE2 sites.

[1]Section of Molecular Biology, Division of Biological Sciences, University of California, San Diego, 9500 Gilman Drive, La Jolla, CA 92093-0322, USA. [2]Laboratory of Cell Biology, National Cancer Institute, National Institutes of Health, Bethesda, MD 20892, USA. [3]Department of Pharmacology, Fox Chase Cancer Center, 333 Cottman Avenue, PA 19111, USA.
[4]Correspondence should be addressed to Y.X. (e-mail: yangxu@ucsd.edu)

Published online: 26 December 2004, DOI: 10.1038/ncb1211

©2005 Nature Publishing Group

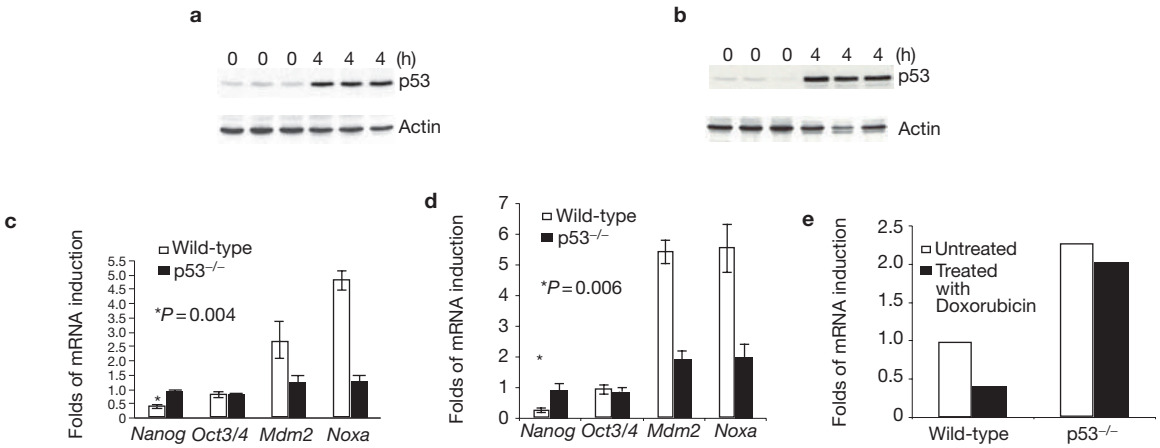

Figure 1 p53-dependent suppression of *Nanog* expression. Induction of p53 protein levels in ESCs 4 h after 60 J M^{-2} UV radiation (**a**) and 0.5 μM Doxorubicin treatment (**b**). The expression of p53 and actin at the indicated time points. Induction of gene expression of *Nanog*, *Oct3/4*, *Mdm2* and *Noxa* in ESCs 4 h after UV radiation (**c**) and Doxorubicin treatment (**d**). The mRNA levels of each gene were determined by quantitative real-time PCR and standardized by the mRNA levels of *GAPDH*. *P* values for *Nanog* expression are shown. (**e**) Suppression of *Nanog* expression in $p53^{+/+}$ and $p53^{-/-}$ blastocysts 6 h after Doxorubicin treatment. The mRNA levels of *Nanog* were determined by quantitative real-time PCR and standardized by the mRNA levels of *GAPDH*. The mRNA levels of *Nanog* in untreated wild-type blastocysts were set to 1.

p53 can suppress gene expression through direct and indirect mechanisms. To determine whether p53 suppresses *Nanog* expression directly, we cloned a 1-kb genomic DNA containing the *Nanog* promoter as well as the same genomic DNA with two p53 consensus binding sites mutated (Δp53) into promoterless luciferase constructs (see Supplementary Information, Fig. S1). Transient transfection of the wild-type and Δp53 luciferase constructs together with a control vector into ESCs or mouse embryonic fibroblasts (MEFs) indicated that the cloned *Nanog* promoter was active in ESCs but not in MEFs (Fig. 2d). Therefore, the regulation of gene expression conferred by the cloned *Nanog* promoter is consistent with the *in vivo* regulation of *Nanog* expression. In addition, the Δp53 promoter was more active than the wild-type *Nanog* promoter in ESCs, indicating that the two p53 consensus binding sites are involved in the suppression of *Nanog* expression in ESCs. The same conclusion was reached when the promoter activities of a 2.5-kb wild-type and Δp53 promoter region of *Nanog* were compared using the luciferase assay (data not shown). The *Nanog* promoter was also active in $p53^{-/-}$ ESCs, but its activities were suppressed when the vector expressing p53 was co-transfected with the *Nanog* promoter luciferase construct into $p53^{-/-}$ ESCs (Fig. 2e). To further test whether the suppression of *Nanog* expression by p53 activated after DNA damage is direct, we analysed the change in the promoter activities of wild-type and Δp53 promoters in ESCs 4 h after Doxorubicin treatment and found that the two p53 consensus binding sites were mediating the p53-dependent suppression of *Nanog* promoter activities (Fig. 2f).

In response to treatment with retinoic acid, mouse ESCs differentiate into cell types resembling those found in early stages of mouse embryogenesis[7]. Consistent with previous findings, p53 protein levels were reduced after retinoic-acid-induced ESC differentiation (Fig. 3a)[8]. By contrast, the transcriptional activity of p53 was increased, and the p53-dependent expression of *p21*, *Mdm2* and *Killer/DR5* were all markedly induced during ESC differentiation (Fig. 3b). Similar findings (of decreased p53 protein levels but increased activity) have been reported for embryonic teratocarcinoma cells[9]. Consistent with the idea that p53 suppresses *Nanog* expression, *Nanog* expression inversely correlated with p53 activity during ESC differentiation (Fig. 3b). As expected, no notable change in the expression of p53-targeted genes was observed in $p53^{-/-}$ ESCs after treatment with retinoic acid (Fig. 3c). However, although mRNA levels of *Nanog* were also reduced in $p53^{-/-}$ ESCs after treatment with retinoic acid, the folds of reduction were smaller than those observed in wild-type ESCs (Fig. 3b, c). Therefore, p53 is involved in the rapid down-regulation of *Nanog* expression during retinoic-acid-induced ESC differentiation.

Phosphorylation of p53 has important roles in the regulation of p53 stability and activity[10]. To understand the mechanism whereby p53 stability and activity are regulated during retinoic-acid-induced ESC differentiation, we profiled the phosphorylation pattern of p53 in ESCs during retinoic-acid-induced differentiation. For this analysis we used ESCs containing a humanized p53 allele, denoted humanized p53 knock-in (p53hki). The p53hki allele encodes a chimeric p53 protein that consists primarily of human p53 (codons 33–332 of human p53) along with the conserved amino and carboxy terminus of mouse p53 (ref. 11). More importantly, p53hki in mouse cells can be considered functionally equivalent to mouse p53 (ref. 11). The rationale for using the p53hki allele is that most of the phospho-specific antibodies for p53 have been raised against the human protein and are specific for human p53. Consistent with the finding that cyclin-dependent kinase (CDK) activity is greatly increased during ESC differentiation[12], phosphorylation of p53 at Ser 315 (which could be mediated by CDK[13,14]) seemed to be the major phosphorylation event during retinoic-acid-induced ESC differentiation (Fig. 3d). In addition, Ser 315 phosphorylation was also detected during ESC differentiation induced by 3′ methoxybenzamide (MBA), suggesting that Ser 315 phosphorylation is a common event during ESC differentiation (data not shown).

To determine whether Ser 315 phosphorylation was required for regulating p53 stability and activity during ESC differentiation, we introduced a missense S315A mutation into the endogenous p53hki allele in the AY ESC line, which harbours one wild-type p53 allele and one p53-deleted allele[15] (see Supplementary Information, Fig. S2). We profiled the phosphorylation pattern of p53 in p53hki and $p53hki^{S315A}$ ESCs after UV radiation and treatment with retinoic acid. The phosphorylation patterns of p53 after DNA damage were similar between

©2005 Nature Publishing Group

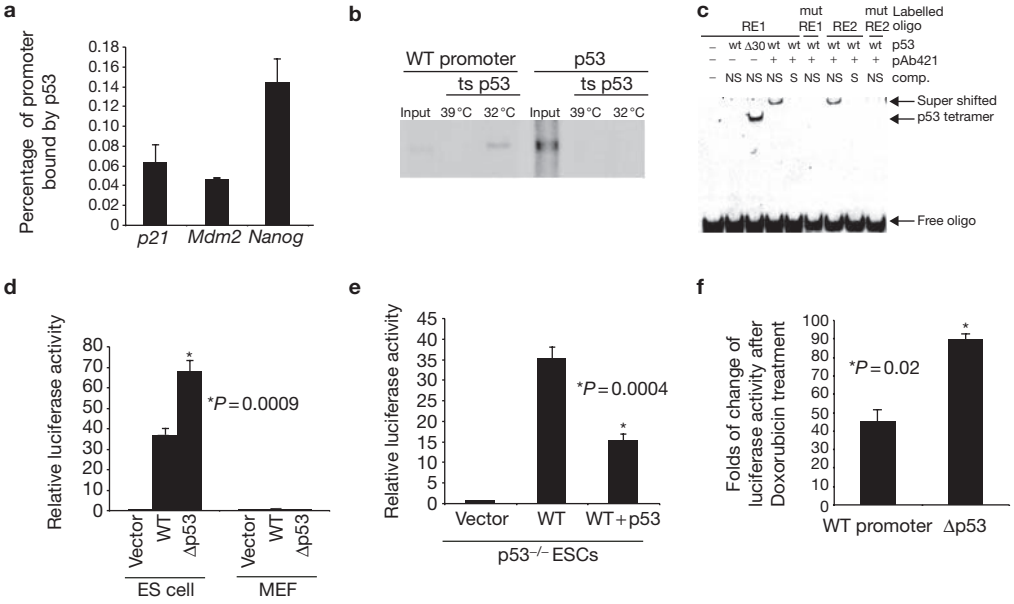

Figure 2 p53 binds to the *Nanog* promoter. (**a**) ChIP analysis of DNA-binding of p53 to p53-dependent promoters and to the *Nanog* promoter in ESCs. The percentage of total promoter bound by p53 was determined by quantitative PCR. The percentage of actin promoter was used as a negative control. The percentage of total actin promoter immunoprecipitated by p53 was 1–2% of that of the *Nanog* promoter. (**b**) The binding of p53 to the 0.7-kb *Hin*dIII fragment harbouring the wild-type or mutated RE1/2 sites was determined by the McKay assay. Temperature-sensitive p53 was used in the binding reaction so that p53 produced at 32 °C but not at 39 °C could bind to p53 consensus binding sites. (**c**) EMSA analysis of the binding of p53 to RE1 and RE2 oligonucleotides. Purified human wild-type p53 (wt) or p53(1–363) (Δ30) was incubated with fluorescent-dye-labelled wild-type or mutant (mut) double-stranded oligonucleotides in the presence of unlabelled specific (S) or non-specific (NS) competitor and, where indicated, pAb421 antibody. The migrating positions of free oligonucleotide (f), bound tetramer (b) and supershifted antibody–p53–DNA complex (ss) are indicated. (**d**) Wild-type and Δp53 promoter activity in ESCs and MEFs. Relative luciferase activity of wt–Luc and Δp53–Luc compared with the promoterless vector is shown. *P* values for the difference between wt–Luc and Δp53–Luc activity in ESCs are shown. (**e**) wt–Luc activity is suppressed by the expression of p53 in $p53^{-/-}$ ESCs. A vector expressing p53 (25 ng) was co-transfected with wt–Luc into $p53^{-/-}$ ESCs. (**f**) The change in the luciferase activity of wt–Luc and Δp53–Luc 4 h after 3 μM Doxorubicin treatment compared with that of untreated samples. Mean values from three independent experiments are shown with error bars (standard deviation).

p53hki and $p53hki^{S315A}$ ESCs (Fig. 3d). Consistent with this finding, p53 stability and activity were similar between p53hki and $p53hki^{S315A}$ ESCs after UV radiation (see Supplementary Information, Fig. S3). However, the phosphorylation patterns of p53 in p53hki and $p53hki^{S315A}$ ESCs after retinoic acid treatment differed at two of the phosphorylation sites analysed. Specifically, Ser 46 and Ser 392 were hyperphosphorylated in $p53hki^{S315A}$ ESCs (Fig. 3d).

Analysis of p53 protein levels after retinoic acid treatment indicated that p53 protein levels were increased in $p53hki^{S315A}$ ESCs during the early stages of retinoic-acid-induced ESC differentiation, instead of being decreased as observed in p53hki ESCs (Fig. 4a, b). Therefore, Ser 315 phosphorylation may have a role in the rapid down-regulation of p53 protein levels during ESC differentiation. Similarly to that in wild-type ESCs, *Nanog* expression was rapidly reduced in p53hki ESCs after retinoic acid treatment (Fig. 4c). However, *Nanog* expression in $p53hki^{S315A}$ ESCs was not notably down-regulated during the initial 48 h after retinoic acid treatment, and was expressed at significantly higher levels than that in p53hki ESCs (Fig. 4c). These data suggest that p53-dependent transcriptional activities were impaired in $p53hki^{S315A}$ ESCs during ESC differentiation. Consistent with this notion, p53-dependent activation of *p21* and *Mdm2* was reduced in $p53hki^{S315A}$ ESCs compared with p53hki ESCs, during ESC differentiation (Fig. 4d). The impaired down-regulation of *Nanog* in $p53hki^{S315A}$ ESCs after treatment with retinoic acid led to resistance of these ESCs to retinoic-acid-induced differentiation, as indicated by the lack of a significant reduction in *Oct3/4* expression, as well as the morphology of $p53hki^{S315A}$ ESCs after treatment with retinoic acid (Fig. 3d; also see Supplementary Information, Fig. S4). In addition, $p53hki^{S315A}$ ESCs were more resistant to ESC differentiation induced by MBA treatment as well as withdrawal of leukaemia inhibitory factor (LIF) (see Supplementary Information, Fig. S4). The combined data indicate that Ser 315 phosphorylation is important in activating p53 transcriptional activities during ESC differentiation, including the rapid suppression of *Nanog* expression.

p53 is known to suppress gene expression by the recruitment of histone deacetylase through the direct interaction of p53 with the co-repressor mSin3a[16]. To elucidate the mechanism for p53-mediated suppression of *Nanog* expression during ESC differentiation, we used ChIP to analyse the p53 binding, histone acetylation and recruitment of mSin3a to the *Nanog* promoter before or after treatment with retinoic acid. Our analysis indicated that, although binding of p53 to the *Nanog* promoter was modestly reduced after treatment with retinoic acid, histone H3 acetylation of the *Nanog* promoter was significantly reduced after treatment with retinoic acid (Fig. 5a). In addition, recruitment of mSin3a to the *Nanog* promoter after retinoic acid treatment was increased (Fig. 5a). Because Ser 315 resides proximal to the DNA-binding domain of p53, we tested the impact of Ser 315 phosphorylation on the *in vivo* DNA binding of p53 to the *Nanog* promoter after treatment with retinoic acid. A similar amount of *Nanog* promoter was bound by p53 in p53hki and $p53hki^{S315A}$ ESCs 48 h after treatment with retinoic acid, indicating that the impaired suppression of *Nanog* in $p53hki^{S315A}$ ESCs after treatment with retinoic acid is not due to reduced binding of p53 to the *Nanog* promoter (Fig. 5b). Consistent with the finding that acetylation of histone 3 in the *Nanog*

©2005 Nature Publishing Group

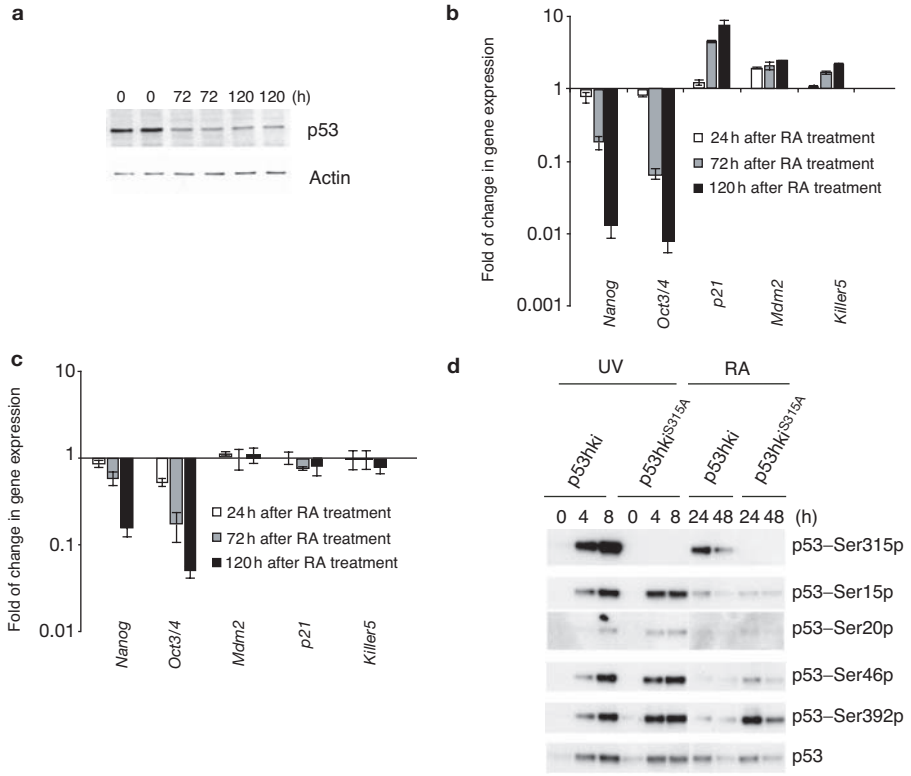

Figure 3 p53 activation and phosphorylation during retinoic-acid-induced ESC differentiation. (**a**) Down-regulation of p53 protein levels during retinoic-acid-induced ESC differentiation. The number of hours after retinoic acid-treatment, p53 and actin are indicated. Change in gene expression of *Nanog*, *Oct3/4*, *p21*, *Mdm2* and *Killer5* in $p53^{+/+}$ (**b**) and $p53^{-/-}$ (**c**) ESCs after retinoic-acid treatment. (**d**) Phosphorylation pattern of p53 during retinoic-acid-induced ESC differentiation. The phosphorylation status of p53 at selected phosphorylation sites in p53hki and p53hki^{S315A} ESCs after UV radiation (left) and during the retinoic-acid-induced differentiation (right). The time points after treatment are indicated on the top. Phosphorylation sites and total p53 are indicated on the right.

promoter was higher in p53hki^{S315A} ESCs than in p53hki ESCs 48 h after treatment, the amount of *Nanog* promoter immunoprecipitated by anti-mSin3a antibody in p53hki^{S315A} ESCs was about half of that in p53hki ESCs, indicating an impaired recruitment of this co-repressor to the *Nanog* promoter (Fig. 5d). Finally, although a marked increase in the interaction between mSin3a and p53 was detected in p53hki ESCs after treatment with retinoic acid, this interaction was greatly decreased in the p53hki^{S315A} cells (Fig. 5e). The combined data support the model whereby phosphorylation of Ser 315 activates p53-dependent suppression of gene expression by promoting the recruitment of the co-repressor mSin3a to the suppressed promoters.

Our findings identify an important role for p53, and specifically the phosphorylation of Ser 315 of p53, in the direct suppression of *Nanog* expression in ESCs. *Nanog* is required for embryonic survival[2]. As the suppression of *Nanog* expression by p53 is partial and $Nanog^{+/-}$ mice are viable[2], these findings could explain why $p53^{-/-}$ mice are still viable. In the absence of Ser 315 phosphorylation, p53 stability is inappropriately increased, but the activity of this protein is decreased, during ESC differentiation. The uncoupling of p53 stability and activity has been well documented in studies of other p53-phosphorylation-site knock-in mutants[17,18]. Consistent with previous observations that phosphorylation of Ser 315 causes a p53 conformational change[14], phosphorylation at the N-terminal (Ser 46) and C-terminal (Ser 392) sites is suppressed by phosphorylation of Ser 315 during ESC differentiation. This role of Ser 315 phosphorylation seems to be process-dependent, because a normal p53 phosphorylation pattern was observed in the absence of Ser 315 phosphorylation after UV irradiation. The roles of Ser 315 phosphorylation include the recruitment of the co-repressor mSin3a to the *Nanog* promoter by promoting mSin3a-p53 interaction.

p53-dependent cell-cycle arrest and apoptosis are not efficient in ESCs after certain types of physiological DNA damage, such as DNA double-strand breaks[19]. Therefore, p53-dependent suppression of *Nanog* expression represents an alternative pathway to maintain genetic stability in ESCs by inducing the differentiation of ESCs into other cell types — such as the differentiated ESCs — that can undergo efficient p53-dependent cell-cycle arrest or apoptosis[19,20]. Our findings could account for some earlier observations. For example, the activation of p53 responses by oncoproteins could explain the observation that activation of Ras in ESCs leads to *Nanog* down-regulation and ESC differentiation[21]. In addition, although ionizing radiation does not induce p53-dependent apoptosis in ESCs, it significantly reduces the clonogenic potential of wild-type ESCs but not $p53^{-/-}$ ESCs[22].

METHODS

ESC culture, treatment and differentiation. ESCs were cultured on a feeder layer in Dulbecco's modified Eagle's medium (DMEM) supplemented with 15% fetal calf serum (FCS), glutamine, non-essential amino acids, antibiotics, 100 μM β-mecaptoethanol and recombinant LIF. To induce DNA damage in ESCs, ESCs were treated with 60 J M^{-2} UV radiation or 0.5 μM Doxorubicin. The differentiation of ESCs *in vitro* was performed as described[20]. Briefly, 1×10^6 ESCs were seeded onto gelatinized 10-cm plates in normal ESC medium. Twenty-four hours after plating, normal ESC medium was changed to the ESC medium without LIF or supplemented with 5×10^{-7} M retinoic acid or 2.5 mM MBA.

©2005 Nature Publishing Group

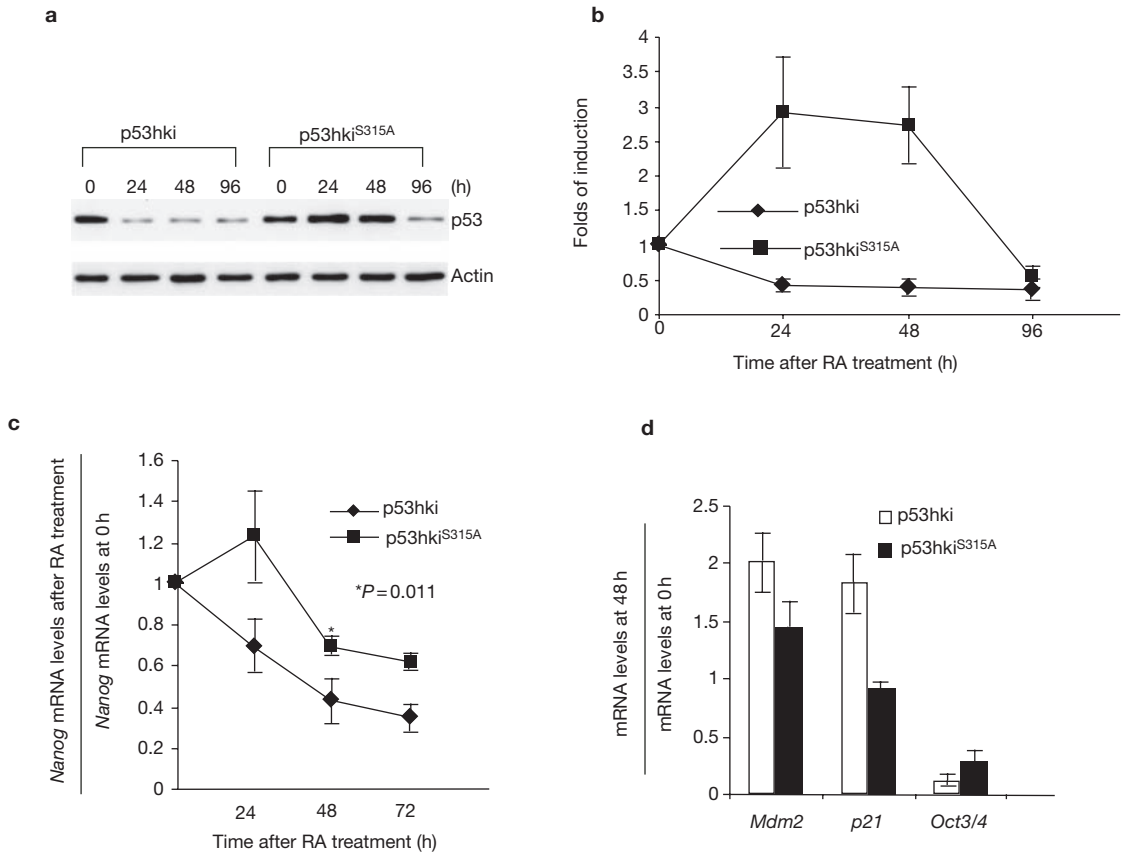

Figure 4 p53 stability and activity in p53hki and p53hki^{S315A} ESCs during retinoic-acid-induced differentiation. (**a**) p53 protein levels at different time points after retinoic-acid-induced differentiation. The genotypes and time points after retinoic acid treatment are shown on top. p53 and actin are shown on the right. (**b**) Statistical analysis of p53 protein levels at different times after retinoic-acid-induced differentiation. (**c**) Quantitative PCR analysis of the change in *Nanog* mRNA expression in p53hki and p53hki^{S315A} ESCs at different times after retinoic-acid-induced ESC differentiation. *P* value 2 days after treatment with retinoic acid is shown. (**d**) Change in mRNA levels of *Mdm2*, *p21* and *Oct3/4* in p53hki and p53hki^{S315A} ESCs 48 h after treatment with retinoic acid.

Alkaline-phosphatase-positive ESC colonies were stained using an ESC kit according to the manufacturer's instructions (Chemicon, Temecula, CA).

***Nanog* promoter construct and luciferase assays for promoter activity.** A 1-kb genomic DNA encompassing the promoter region of *Nanog* was cloned into a promoterless luciferase construct, pGL3Basic vector (Promega, Madison, WI). The C/G to A/T mutations at the consensus p53-binding sites were introduced by site-directed mutagenesis. Luciferase assays were performed using the Dual Luciferase system (Promega). ESCs were plated at a density of 5×10^4 cells per well of a 24-well plate. Wild-type and mutant promoter luciferase constructs (25 ng of each) were transfected into ESCs with a control vector by Lipofectamine according to the manufacturer's instructions (Invitrogen, Carlsbad, CA). Twenty fours after transfection, the luciferase activities were analysed using the Dual Luciferase system. For analysis of luciferase activities after DNA damage, transfected ESCs were treated with 3 M Doxorubicin for 4 h before harvesting for analysis. For the co-transfection experiment, full-length mouse p53 cDNA was cloned into an expression vector that drives gene expression in ESCs.

Construction of p53hki^{S315A} ESCs. Ser 315 is encoded by exon 9 of human p53 and the missense mutation (S315A) was introduced into exon 9 of the human p53 genomic DNA in the targeting vector by site-directed mutagenesis as described (see Supplementary Information, Fig. S1b). The targeting vector is the same as described previously[11]. To facilitate the mutagenesis processes, the knock-in construct was electroporated into a p53$^{+/-}$ ESC line (AY ESCs) that was described previously[15] (see Supplementary Information, Fig. S1a). As a positive control, the targeting vector with the wild-type human p53 exons was also electroporated into AY ESCs. Homologous recombination between the knock-in vectors and the sole germline mouse p53 allele in AY ESCs replaced exons 4–9 of mouse p53 with exons 4–9 of human p53 that were either wild-type or harboured the S315A mutation. The homologous recombinants were screened by PCR with primers 1 and 2 and confirmed by Southern blot analysis with *Bgl*II digestion and hybridization to probe A, giving rise to a 15-kb germline band and an 8-kb mutant band (see Supplementary Information, Fig. S1c, e). The PGK–neo^r/TK cassette was excised from the targeted allele through *LoxP*/Cre-mediated deletion (see Supplementary Information, Fig. S2d). The deletion was screened by PCR with primers (see Supplementary Information, Fig. S1d) and confirmed by Southern blot analysis with *Eco*RI digestion (see Supplementary Information, Fig. S1d). ESCs with p53 containing the wild-type human p53 exons are denoted 'p53hki ESCs', whereas those with the S315A mutation are denoted 'p53hki^{S315A} ESCs'.

Western blot analysis. Protein extracts from 5×10^6 ESCs were separated by SDS–PAGE on a 10% polyacrylamide gel and transferred to nitrocellulose membrane. The membrane was blocked with 5% dry milk and probed with a monoclonal antibody against p53 (pAb1801; Santa Cruz Biotechnology, Santa Cruz, CA) or a polyclonal antibody against p53 (CM-5; Vector Laboratories, Burlingame, NH). The filter was then incubated with a horseradish-peroxidase-conjugated secondary antibody and developed with enhanced chemilluminescence PLUS reagent from Amersham (Piscataway, NJ). To determine that the amount of protein in each lane was comparable, the filter was stripped and probed with a rabbit polyclonal antibody against β-actin (Santa Cruz Biotechnology).

Immunoprecipitation and western blot analysis of Sin3–p53 complex formation. Cells were treated with retinoic acid for 48 h as described above, and after harvesting, were lysed in 2 ml of NP-40 lysis buffer supplemented with protease inhibitors, as described[16]. Samples containing 400 μg of whole-cell lysate were incubated with 2.5 μg of anti-mSin3a antibody (1.25 μg each of AK-11 and K-20; Santa Cruz Biotechnology) for 2 h, followed by incubation with 30 μl of 50% (v/v) protein-A sepharose beads (Sigma, St Louis, MO) for 30 min. Immunocomplexes

©2005 Nature Publishing Group

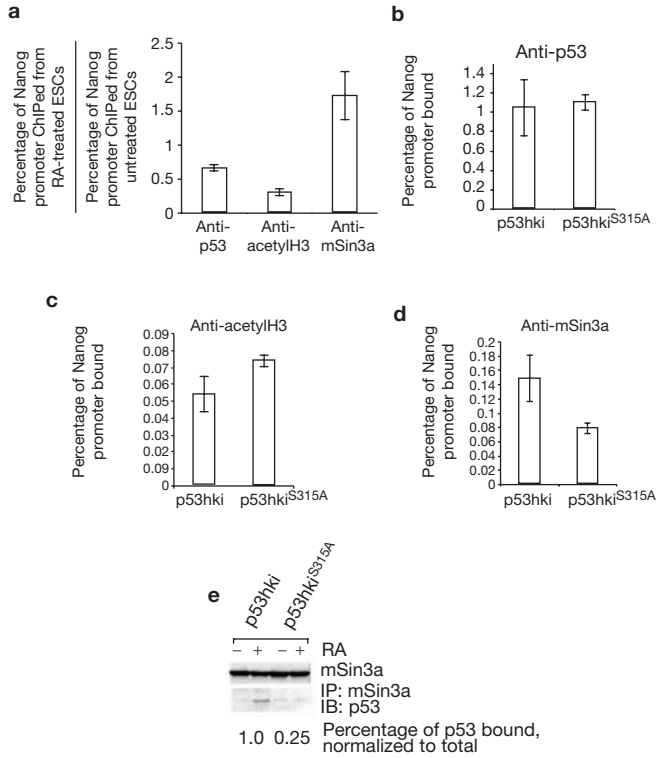

Figure 5 Recruitment of co-repressor mSin3a to the *Nanog* promoter. (**a**) Change in p53 binding, acetylation of histone H3 and the recruitment of mSin3a to the *Nanog* promoter before and 48 h after treatment with retinoic acid in wild-type ESCs. ChIP analysis of DNA-binding of p53 (**b**), acetylation of histone (**c**), and recruitment of mSin3a (**d**) to the *Nanog* promoter in p53hki and p53hki^{S315A} ESCs 48 h after retinoic acid treatment. The amount of *Nanog* promoter fragments in the immunoprecipitate and input was determined by quantitative real-time PCR. The percentage of total *Nanog* promoter immunoprecipitated by anti-p53, anti-acetylated histone H3 and anti-mSin3a antibodies is shown. (**e**) Interaction of p53 and mSin3a by co-immunoprecipitation (IP) and immunoblotting (IB). Genotypes and treatment are shown on the top. p53 and mSin3a are labelled on the right.

were washed twice in NP-40 lysis buffer and once in RIPA buffer as described[16], before 30 µl of 2× Laemmli sample buffer was added and complexes resolved on 10% SDS–PAGE gels (NuPAGE; Invitrogen). After overnight transfer, blots were probed with goat antibody to p53 (E19; Santa Cruz Biotechnology) or anti-Sin3 (AK-11 and K-20; Santa Cruz Biotechnology).

Real-time PCR analysis. Total RNA was isolated from ESCs with the combination of Trizol (Invitrogen) and RNAeasy RNA Cleanup (Qiagen, Valencia, CA). RNA was treated with RNase-free DNAse for 20 min (Roche, Basle, Switzerland) at room temperature before reverse transcription with Superscript II RT (Invitrogen). Real-time PCR was performed on an ABI 7000 machine with SyBr Green PCR Master Mix (ABI, Foster City, CA). PCR conditions consisted of a 10 min hot start at 95 °C, followed by 40 cycles of 30 s at 95 °C and 1 min at 61 °C. The average threshold cycle (Ct) for each gene was determined from triplicate reactions and the levels of gene expression relative to GAPDH were determined as described[23]. The primer sequences for *p21*, *Mdm2*, *Noxa*, *Perp*, *Killer 5* and *GAPDH* were described previously[18]. Other primers are as follows: *Nanog*, 5′-CAGAAAAA CCAGTGGTTGAAGACTAG-3′ and 5′-GCAATGGATGCTGGGATACTC-3′; and *Oct3/4*, 5′-TGAGAACCTTCAGGAGATATGCAA-3′ and 5′-CTCAATGC TAGTTCGCTTTCTCTTC-3′.

Blastocyst harvest and treatment. To harvest p53$^{+/+}$ and p53$^{-/-}$ blastocysts, p53$^{+/+}$ or p53$^{-/-}$ females in estrus were set up with p53$^{+/+}$ or p53$^{-/-}$ males, respectively. Three and half days after the plug, blastocysts were harvested from the uterus of the plugged female. Pooled p53$^{+/+}$ or p53$^{-/-}$ blastocysts were untreated or treated with 3 µM Doxorubicin in M2 medium for 6 h before total RNA was isolated from treated and untreated samples by RNAeasy RNA Cleanup (Qiagen). The mRNA levels of *Nanog* and *GAPDH* were determined by quantitative real-time PCR as described above.

McKay assay. A McKay assay to detect the sequence-specific DNA binding of p53 to the DNA fragment of the *Nanog* promoter was performed as described[6]. Briefly, cells expressing temperature-sensitive p53 were cultured at 39 °C or 32 °C for 24 h and lysed in 1 ml of McKay binding buffer (10% glycerol, 5 mM EDTA, 20 mM Tris at pH 7.2, 100 mM NaCl, 0.1% NP-40 and protease inhibitors). After spinning at 16,000*g* for 10 min at 4 °C, the supernatant was collected and the protein concentration determined using the Bio-Rad DC assay. Aliquots containing 100 µg of protein were incubated with the radiolabelled DNA fragment containing the consensus p53-binding sites, 0.5 µg of p53 polyclonal antibody (FL-393; Santa Cruz Biotechnology), poly dI/dC and 30 µl of protein-A sepharose (50% v/v, equilibrated in binding buffer). After rotation for 30 min at 4 °C, immunoprecipitates were collected, washed and resolved on a 4% non-denaturing acrylamide gel. After electrophoresis, the gel was dried and exposed to X-ray film.

Electrophoretic mobility shift assay. The sequences of the oligonucleotides used to test for binding of p53 are as follows: RE1, 5′-TAAATTGGGCATGGTGGTA GACAAGCCTGGTCTACA-3′; and RE2, 5′-TTTGGCAGCAAGGTCTGACTC TTTCATGTCTGTAG-3′; and their corresponding complementary sequences. The mutated versions of the sequences were: mutRE1, 5′-TAAATTGGGGATCG TGGTAGAGAACCCTGGTCTACA-3′; and mutRE2, 5′-TTTGGCAGGAACG TCTGAGTCTTTGATCTCTGTAG-3′. Oligonucleotides were gel purified. The strands shown above were synthesized with a 5′ amino modification whereas the complementary strands were unmodified. Labelled oligonucleotides were prepared by reaction with the Alexa Fluor 647 dye (Molecular Probes, Eugene, OR) according to the manufacturer's instructions and purified by polyacrylamide gel electrophoresis. Double-stranded oligonucleotides were prepared by annealing equimolar amounts of the bottom strand with labelled or unlabelled top strand. Binding reactions were performed in a buffer containing 25 mM Na-HEPES (at pH 7.5), 50 mM KCl, 0.1% NP40, 1 mM dithiothreitol, 10% glycerol and 1 mg ml^{-1} bovine serum albumin. Purified wild-type p53 and p53Δ30 were obtained from ProteinOne (College Park, MD). Wild-type p53 was activated by incubation with the pAb421 antibody for 15 min on ice. Binding reactions typically contained 2 nM labelled double-stranded oligonucleotide, 100 nM non-specific or specific competitor, 20 nM (monomer) p53 and, if indicated, 100 ng µl^{-1} of pAb421. An unlabelled, double-stranded *p21* 30-nucleotide-long sequence was used as the specific competitor and unlabelled, double-stranded mutRE2 was used as the non-specific competitor. Reactions were incubated for 20 min at room temperature. The products were subjected to electrophoresis through a 5% polyacrylamide, 0.5 × TBE gel at 6 V cm^{-1} at 4 °C while protected from light. The gels were scanned with a Storm imager (Molecular Dynamics, Piscataway, NJ) using the red fluorescence mode.

Chromatin immunoprecipitation assay. ChIP analysis of *in vivo* binding of p53 to p53-dependent promoters was performed essentially as described[18]. For ChIP, 5 × 10^6 ESCs or differentiated ESCs were fixed with 1% formaldehyde for 10 min at room temperature. Formaldehyde was neutralized by the addition of 125 mM glycine for 5 min. Cells were washed twice in ice-cold PBS and lysed in 0.5 ml of lysis buffer (0.25% SDS, 200 mM NaCl, 50 mM Tris at pH 8.0, 100 mg l^{-1} of sonicated salmon sperm DNA and protease inhibitors) and sonicated to an average fragment size of 0.6 kb using a microtip. Remaining insoluble material was removed by centrifugation at 4 °C for 10 min. The supernatant was diluted with two volumes of 1% NP-40, 350 mM NaCl and precleared with normal mouse IgG and protein A-agarose beads. Each ChIP sample was incubated for 12 h at 4 °C with 1 µg of monoclonal antibodies against p53 (Pab421 or PAB1801; Santa Cruz Biotechnology), polyclonal antibody against acetylated H3 (Upstate, Lake Placid, NJ) or mSin3a (Santa Cruz Biotechnology). Immune complexes were collected with protein A-agarose beads and cross-linking was reversed by incubation of the eluate overnight at 65 °C. After digestion with 160 mg l^{-1}. Proteinase K and incubation for 1 h at 55 °C, DNA was purified by extraction with phenol–chloroform and precipitated with isopropanol and glycogen. The amounts of DNA in the immunoprecipitates and the input were quantified by real-time PCR. The ChIP data are reported as the percentage of total input promoter that was immunoprecipitated. Quantitative PCR was performed on an ABI7000 PCR machine using an SYBR Master Mix (Perkin Elmer, Norwalk, CT). The sequence

©2005 Nature Publishing Group

of PCR steps used was 50 °C for 2 min to digest dUTP-containing DNA, 95 °C for 10 min to activate Taq Gold polymerase, followed by cycles of 95 °C for 15 s and 60 °C for 1 min, repeated 40 times. The primer sequences for *p21* and *Mdm2* promoters were described previously[18]. The primer sequences for *Nanog* promoter are as follows: 5′-CAACTTACTAAGGTAGCCCGAGTCTTAA-3′ and 5′-CCTCCAAAAGTGCGGCTTT-3′.

BIND identifiers. Seven BIND identifiers (www.bind.ca) are associated with this manuscript: 193087, 193088, 193089, 193090, 193091, 193092, 193094

Note: Supplementary Information is available on the Nature Cell Biology website.

ACKNOWLEDGEMENTS
This work was supported by a National Institutes of Health grant (CA94254) to Y.X. We thank M. Hollstein for the humanized p53 knock-in construct and H. Niwa for the episomal expression vector that expresses in ESC.

COMPETING FINANCIAL INTERESTS
The authors declare that they have no competing financial interests.

Received 19 August 2004; accepted 22 November 2004
Published online at http://www.nature.com/naturecellbiology.

1. Ko, L. J. & Prives, C. p53: puzzle and paradigm. *Genes Dev.* **10,** 1054–1072 (1996).
2. Mitsui, K. *et al.* The homeoprotein Nanog is required for maintenance of pluripotency in mouse epiblast and ES cells. *Cell* **113,** 631–642. (2003).
3. Chambers, I. *et al.* Functional expression cloning of Nanog, a pluripotency sustaining factor in embryonic stem cells. *Cell* **113,** 643–655 (2003).
4. Okamoto, K. *et al.* A novel octamer binding transcription factor is differentially expressed in mouse embryonic cells. *Cell* **60,** 461–472 (1990).
5. Niwa, H., Miyazaki, J. & Smith, A. G. Quantitative expression of Oct-3/4 defines differentiation, dedifferentiation or self-renewal of ES cells. *Nature Genet.* **24,** 372–376 (2000).
6. Hoffman, W. H., Biade, S., Zilfou, J. T., Chen, J. & Murphy, M. Transcriptional repression of the anti-apoptotic survivin gene by wild type p53. *J. Biol. Chem.* **277,** 3247–3257 (2002).
7. Rohwedel, J., Guan, K. & Wobus, A. M. Induction of cellular differentiation by retinoic acid *in vitro*. *Cells Tissues Organs* **165,** 190–202 (1999).
8. Sabapathy, K., Klemm, M., Jaenisch, R. & Wagner, E. F. Regulation of ES cell differentiation by functional and conformational modulation of p53. *EMBO J.* **16,** 6217–6229 (1997).
9. Lutzker, S. G. & Levine, A. J. A functionally inactive p53 protein in teratocarcinoma cells is activated by either DNA damage or cellular differentiation, *Nature Med.* **2,** 804–810 (1996).
10. Xu, Y. Regulation of p53 responses by post-translational modifications, *Cell Death Differ.* **10,** 400–403 (2003).
11. Luo, J. L., *et al.* Knock-in mice with a chimeric human/murine *p53* gene develop normally and show wild-type p53 responses to DNA damaging agents: a new biomedical research tool, *Oncogene* **20,** 320–328 (2001).
12. Savatier, P., Lapillonne, H., van Grunsven, L. A., Rudkin, B. B. & Samarut, J. Withdrawal of differentiation inhibitory activity/leukemia inhibitory factor up-regulates D-type cyclins and cyclin-dependent kinase inhibitors in mouse embryonic stem cells. *Oncogene* **12,** 309–322 (1996).
13. Bischoff, J. R., Friedman, P. N., Marshak, D. R., Prives, C. & Beach, D. Human p53 is phosphorylated by p60–cdc2 and cyclin B–cdc2. *Proc. Natl Acad. Sci. USA* **87,** 4766–4770 (1990).
14. Wang, Y. & Prives, C. Increased and altered DNA binding of human p53 by S and G2/M but not G1 cyclin-dependent kinases. *Nature* **376,** 88–91 (1995).
15. Wu, Z. *et al.* Mutation of mouse p53 Ser23 and the response to DNA damage. *Mol. Cell. Biol.* **22,** 2441–2449 (2002).
16. Murphy, M. *et al.* Transcriptional repression by wild-type p53 utilizes histone deacetylases, mediated by interaction with mSin3a. *Genes Dev.* **13,** 2490–2501 (1999).
17. Chao, C. *et al.* p53 transcriptional activity is essential for p53-dependent apoptosis following DNA damage, *EMBO J.* **19,** 4967–4975 (2000).
18. Chao, C. *et al.* Cell type- and promoter-specific roles of Ser18 phosphorylation in regulating p53 responses. *J. Biol. Chem.* **278,** 41028–41033 (2003).
19. Aladjem, M. I. *et al.* ES cells do not activate p53-dependent stress responses and undergo p53-independent apoptosis in response to DNA damage. *Curr. Biol.* **8,** 145–155 (1998).
20. Chao, C., Saito, S., Anderson, C. W., Appella, E. & Xu, Y. Phosphorylation of murine p53 at ser-18 regulates the p53 responses to DNA damage. *Proc. Natl Acad. Sci. USA* **97,** 11936–11941 (2000).
21. Yoshida-Koide, U. *et al.* Involvement of Ras in extraembryonic endoderm differentiation of embryonic stem cells. *Biochem. Biophys. Res. Commun.* **313,** 475–481 (2004).
22. Corbet, S. W., Clarke, A. R., Gledhill, S. & Wyllie, A. H. P53-dependent and -independent links between DNA-damage, apoptosis and mutation frequency in ES cells. *Oncogene* **18,** 1537–1544 (1999).
23. Boley, S. E., Wong, V. A., French, J. E. & Recio, L. p53 heterozygosity alters the mRNA expression of p53 target genes in the bone marrow in response to inhaled benzene. *Toxicol. Sci.* **66,** 209–215 (2002).

©2005 Nature Publishing Group

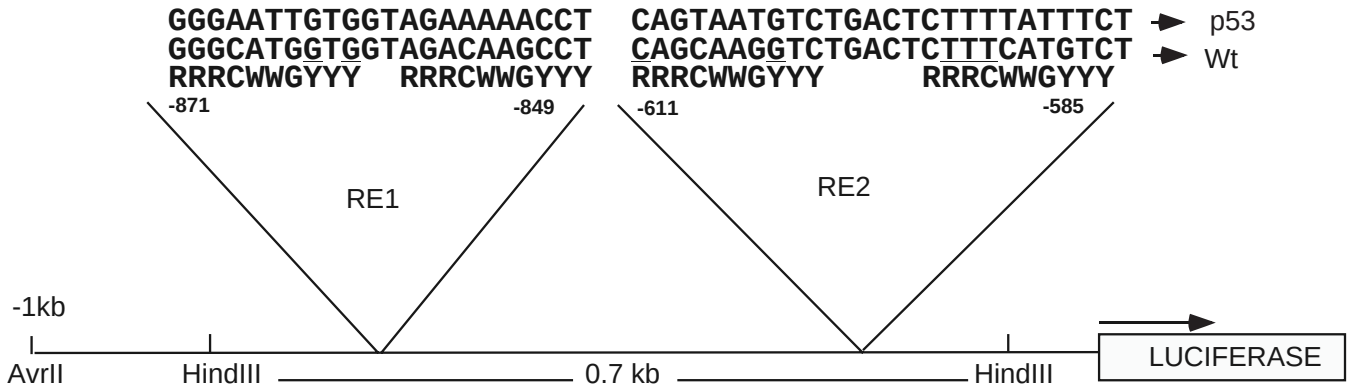

Figure S1 The promoter region of Nanog. The positions and sequence of the two p53 DNA-binding sites are shown, with deviations from the consensus sequence underlined. The consensus p53-binding site consists of two copies of the 10 base pair (bp) motif 5'-PuPuPuC(A/T)(T/A)GPyPyPy-3' separated by 0 to 13 bps. The consensus p53 binding sites were mutated by replacing the critical C/G residues with A/T in the construction of luciferase reporters. One kb genomic DNA of Nanog promoter region containing the wild type or mutated p53 consensus DNA binding sites were cloned into a promoterless luciferase construct (Wt-Luc and Dp53-Luc). The transcriptional direction is indicated by arrowhead.

© 2005 Nature Publishing Group

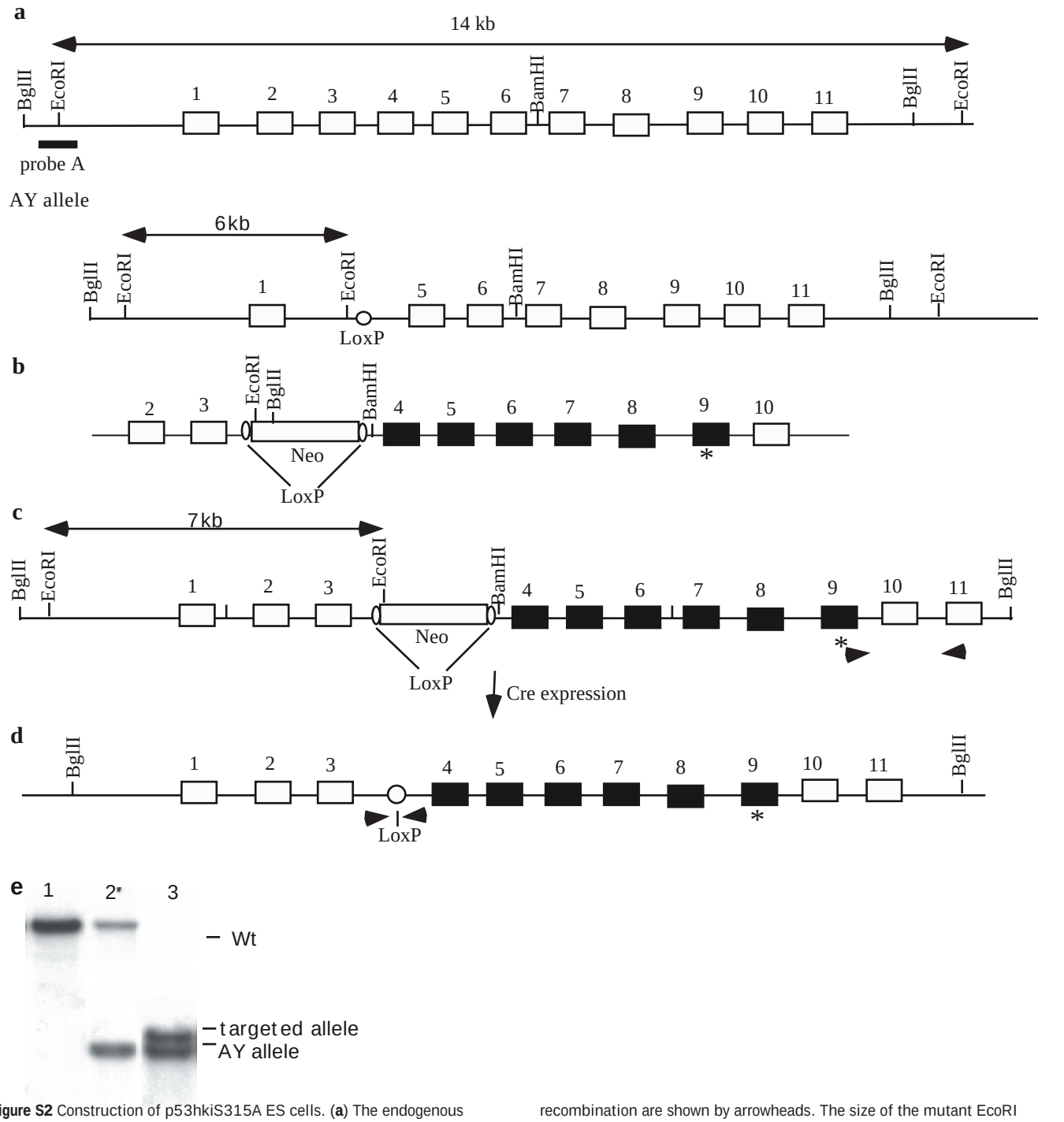

Figure S2 Construction of p53hkiS315A ES cells. (**a**) The endogenous configuration of the p53 gene in AY ES cells. AY ES cells have one wild-type p53 allele and one mutant p53 allele (AY allele) with exons 2-4 deleted. AY allele produces no truncated p53 proteins. Open boxes represent the p53 exons and filled box probes for Southern blot analysis. The size of the EcoRI fragments is indicated. (**b**) The targeting vector. The S315A mutation is indicated by an asterisk. (**c**) Targeted p53 locus after homologous recombination between the wild-type p53 allele and the targeting vector. The positions of the PCR primers used to screen for homologous recombination are shown by arrowheads. The size of the mutant EcoRI fragment is indicated. (**d**) Targeted p53 locus after the PGK-neor gene was deleted through LoxP/Cre-mediated deletion. The positions of the primers that were used to screen for LoxP/Cre-mediated deletion are indicated with arrowheads. (**e**) Southern blot analysis of the genomic DNA derived from wild-type (lane 1), AY (lane 2) and p53hkiS315A (lane 3) ES cells. Genomic DNA was digested with HindIII and hybridized to probe A. The wild-type allele, AY allele and targeted allele are indicated on the right.

© 2005 Nature Publishing Group

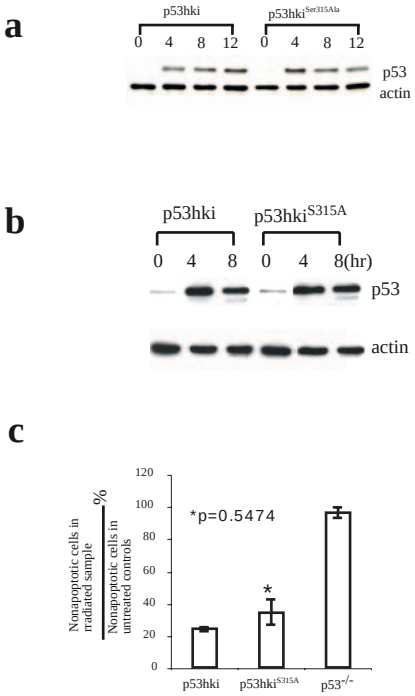

Figure S3 p53 stability and activity in p53hki and p53hkiS315A ES cells after treatment with UV radiation and Doxorubicin. The proteins levels of p53 at different time points after UV radiation (**a**) and Doxorubicin treatment (**b**). The genotype and time points are shown on the top. p53/actin are indicated on the right. (**c**) p53-dependent apoptosis in ES cells after UV radiation. Mean value from four independent experiments is presented with error bars.

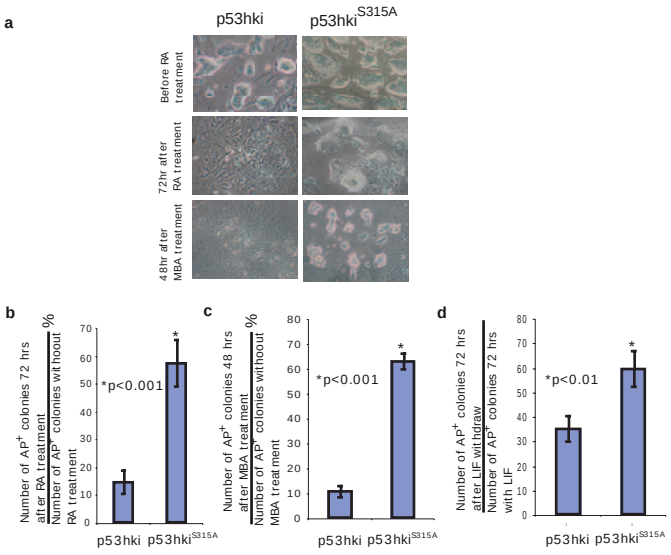

Figure S4 (**a**) ES cell morphology without treatment (top panel), 72 hours after RA treatment (middle panel) or 48 hours after MBA treatment (bottom panel). The genotypes are indicated on the top. The percentages of alkaline phosphtase positive (AP+) ES cell colonies 72 hours after RA treatment (**b**) or 48 hours after MBA treatment (**c**) or 72 hrs after LIF withdraw(**d**) when compared with those in untreated samples.

© 2005 Nature Publishing Group